Evaluating the adsorption capacity of antimony(III) on palygorskite

Marina Campos-Ballesteros (1), Esther Álvarez-Ayuso (1*)

(1) Department of Environmental Geochemistry. IRNASA (CSIC), 37008 Salamanca (Spain)
* corresponding author: esther.alvarez@irnasa.csic.es

Palabras Clave: Palygorskita, Sb, Adsorción, Grupos silanol y aluminol. **Key Words:** Palygorskite, Sb, Adsorption, Silanol and aluminol groups.

INTRODUCTION

The increasing release of antimony (Sb) into the environment has raised concern due to its potential toxic effects on ecosystems and human health. To better understand its environmental behavior and to propose measures for its attenuation, the adsorption properties of different minerals toward this metalloid have become an important focus of study. Metal (oxyhydr)oxides, particularly those of iron, aluminum, and manganese (Bai et al., 2017; Sun et al., 2019; Xiang et al., 2025), along with clay minerals containing reactive aluminol groups such as kaolinite, montmorillonite, and nontronite (Xi et al., 2011, 2016; Ilgen and Trainor, 2012), have received the most attention. While the adsorptive behavior of metal (oxyhydr)oxides is well established, being considered the most important sinks for Sb in impacted environments, the adsorption performance of certain clay minerals remains largely unexplored. This is the case of palygorskite, a magnesium aluminosilicate with a one-dimensional rod-like morphology and a 2:1 (tetrahedral–octahedral–tetrahedral) structure in which periodic inversion of the tetrahedral chains creates a discontinuity in the octahedral sheet aligned with the elongation direction, and generates numerous reactive silanol groups (Wang and Wang, 2019). In addition, partial substitution of magnesium by aluminum in the octahedral sheet produces a significant population of aluminol groups. These metal-bound hydroxyl groups are known to actively adsorb Sb through the formation of inner-sphere complexes (Ilgen and Trainor, 2012). The main objective of this study was to determine the adsorption capacity of Sb(III) on natural palygorskite.

MATERIALS AND METHODS

The palygorskite used in this study originated from Bercimuel (Segovia, Spain) and was provided by MYTA, S.A. (SAMCA Group). Prior to the adsorption experiments, the material was characterized to determine its mineralogical composition, specific surface area (SSA), and point of zero net proton charge (PZNPC). Mineralogical identification was performed by X-ray powder diffraction (XRD) using a Bruker D8 Advance diffractometer, the SSA was measured by the single-point method with a Micromeritics FlowSorb II 2300 analyzer, and the PZNPC was determined following the titration procedure of Van Raij and Peech (1972). To obtain the adsorption isotherm of Sb(III) on palygorskite, batch adsorption experiments were conducted in 50-mL polypropylene flasks. Suspensions containing 5 g/L of palygorskite and Sb(III) solutions of defined concentrations (1–30 mg/L), previously adjusted to pH 8, were equilibrated under continuous agitation on a rotary shaker in a thermostatic chamber set at 22 °C. After equilibration, the solid phase was separated by centrifugation (4000 rpm, 10 min) and Sb concentrations in the supernatants were quantified by inductively coupled plasma–atomic emission spectrometry using a Varian 720-ES instrument.

RESULTS AND DISCUSSION

As determined by XRD (Fig. 1), the palygorskite sample consisted mainly of palygorskite, together with muscovite, quartz, calcite, and smectite. Its SSA and PZNPC were 158 m^2/g and 8.1–8.2, respectively. The adsorption isotherm obtained for Sb(III) removal by the palygorskite sample is shown in Fig. 2. According to the classification of Giles et al. (1960), the isotherm for Sb(III) adsorption on palygorskite within the studied Sb(III) concentration range corresponds to a C-type (constant partitioning). A linear relationship was observed between the equilibrium concentrations (Ce) of Sb(III) in solution and the Sb(III) adsorbed amounts (X/M) on palygorskite [$R^2 = 0.9827$ ($p < 0.001$)]. The distribution coefficient (Kd), calculated as (X/M)/Ce, was 0.110 L/g. The maximum adsorption capacity reached within the studied Sb(III) concentration range was 2.18 mg/g. This value lies within the upper range of maximum adsorption capacities (0.084-3.29 mg/g) reported for Sb(III) at pH 5.5–8 on other clay minerals containing variable amounts of aluminol groups (Xi et al., 2011, 2016; Ilgen and Trainor, 2012). Because Sb(III) occurs predominantly as the neutral species $Sb(OH)_3^0$ between pH 2 and 10 (Filella et al., 2002), the adsorption of Sb(III) on palygorskite is not expected to change significantly within this pH range, despite the change in the palygorskite surface charge above and below its PZNPC.

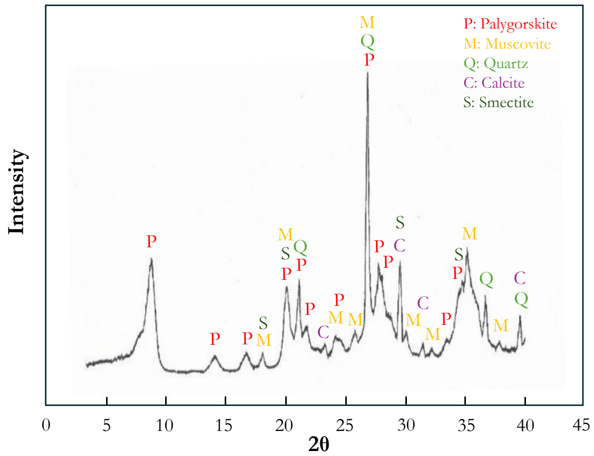

Fig 1. XRD pattern of palygorskite sample.

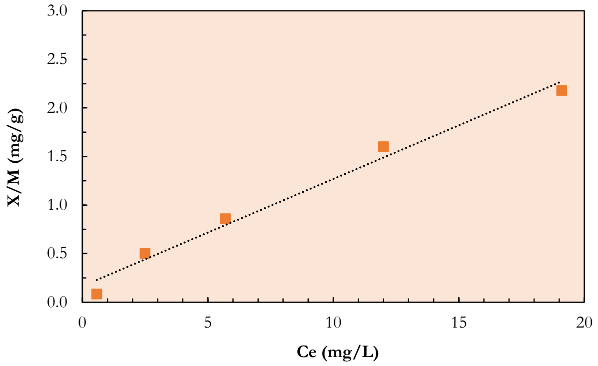

Fig 2. Adsorption isotherm of Sb(III) on palygorskite.

ACKNOWLEDGMENTS

The present study was carried out under the project PURVAL (Grant number: PID2022-141352OB-I00) funded by Ministerio de Ciencia e Innovación (MCIN), Spain/Agencia Estatal de Investigación (AEI), Spain/Fondo Europeo de Desarrollo Regional (FEDER) "A way of making Europe", European Union (EU) and the project “CLU-2019-05 – IRNASA/CSIC Unit of Excellence” funded by the Junta de Castilla y León (Spain) and cofinanced by the EU [European Regional Development Fund (ERDF) “Europe drives our growth”].

REFERENCES

Bai, Y., Jefferson, W.A., Liang, J., Yang, T., Qu, J. (2017): Antimony oxidation and adsorption by in-situ formed biogenic Mn oxide and Fe–Mn oxides. J. Environ. Sci., **54**, 126–134.

Filella, M., Belzile, N., Chen, Y.W. (2002): Antimony in the environment: a review focused on natural waters: II. Relevant solution chemistry. Earth-Sci. Rev., **59**, 265–285.

Giles, C.H., McEwans, T.H., Nakhwa, S.N., Smith, D. (1960): Studies in adsorption: Part IX. A system of classification of solution adsorption isotherms and its use on diagnosis of adsorption mechanisms and in measurement of specific areas of soils. J. Chem. Soc., **786**, 3973–3993.

Ilgen, A.G., Trainor, T.P. (2012): Sb(III) and Sb(V) sorption onto Al-rich phases: Hydrous Al oxide and the clay minerals kaolinite KGa-1b and oxidized and reduced nontronite NAu-1. Environ. Sci. Technol., **46**, 843–851.

Sun, Q., Cui, P.-X., Liu, C., Peng, S.-M., Alves, M.E., Zhou, D.-M., Shi, Z.-Q., Wang, Y.-J. (2019): Antimony oxidation and sorption behavior on birnessites with different properties (Δ-MnO_2 and triclinic birnessite). Environ. Pollut., **246**, 990–998.

Van Raij, B., Peech, M. (1972): Electrochemical properties of some oxisols and alfisols of the tropics. Soil Sci. Soc. Am. J., **36**, 539–695.

Wang, A., Wang, W. (2019): Nanomaterials from clay minerals-A new approach to green functional materials. Elsevier. Cambridge, 693 p.

Xi, J., He, M., Kong, L. (2016): Adsorption of antimony on kaolinite as a function of time, pH, HA and competitive anions. Environ. Earth Sci., **75**, 1–7.

—, —, Lin, C. (2011): Adsorption of antimony(III) and antimony(V) on bentonite: Kinetics, thermodynamics and anion competition. Microchem. J., **97**, 85–91.

Xiang, S., Fu, Z., Lu, H., Sun, Y., Shen, Y., Wu, F. (2025): Antimony and arsenic interactions with iron oxides and aluminum oxides in surface environment: A review focused on processes and mechanisms. Sci. Total Environ., **979**, 179423.